International Tables for Crystallography (2006). Vol. C, Figure 2.7.5.2, p. 122.

stationary slit selecting the beam that it is desired to record, and film, *F*, and interferometer, *SMA*, together traverse to and fro as indicated by the double-headed arrow. In Fig. 2.7.5.1, *S*, *M*, and *A* are the three equally thick wafers of the interferometer that remain upstanding above the base of the monolithic interferometer after the gaps between *S* and *M*, and *M* and *A*, have been milled away. The elements *S*, *M* and *A* are called the splitter, mirror, and analyser, respectively. The moiré pattern is formed between the Bragg planes of *A* and the standing-wave pattern in the overlapping $\mathbf{K}_0$ and $\mathbf{K}_h$ beams entering it. Maximum fringe visibility occurs in the emerging beam that the slit *Q* is shown selecting. A dislocation will appear in the moiré pattern whether the lattice dislocation lies in *S*, *M*, or *A*, provided $\mathbf{b}\cdot\mathbf{h}\neq 0$. Moiré patterns formed in a number of Bragg reflections whose normals lie in, or not greatly inclined to, the plane of the wafers, can be recorded by appropriate orientation of the monolith. By this means, it is easily discovered in which wafer the dislocation lies, and its Burgers vector can be completely determined, including its sense, the latter being found by a deliberate slight elastic deformation of the interferometer (Hart, 1972). Satisfactory moiré topographs have been obtained with an interferometer in a synchrotron beam, despite thermal gradients due to the local intense irradiation (Hart, Sauvage & Siddons, 1980).

Fig. 2.7.5.2 shows crystal slices (1), *ABCD*, and (2), *EFGH*, superposed and simultaneously Bragg reflecting in the Brádler–Lang (1968) method of X-ray moiré topography. The slices could have been cut from separate crystals. In the case when the Bragg planes of (1) and (2) are in identical orientation but have a translational mismatch across *CD* and *EF* with a component parallel to **h**, strong scattering occurs towards *Z* as focus, producing extra intensity at *T′* in the $\mathbf{K}_0$ beam *TT″* and at *R′* in the $\mathbf{K}_h$ beam *RR″*. It is usual to record the moiré pattern using the $\mathbf{K}_h$ beam. Projection moiré topographs are obtained by the standard procedure of traversing the crystal pair and film together with respect to the incident beam *SO*. The special procedure devised for mutually aligning the two crystals so that $\mathbf{h}_1$ and $\mathbf{h}_2$ coincide within their angular range of reflection is explained by Brádler & Lang (1968). This method has been applied to silicon and to natural (Lang, 1968) and synthetic quartz (Lang, 1978).

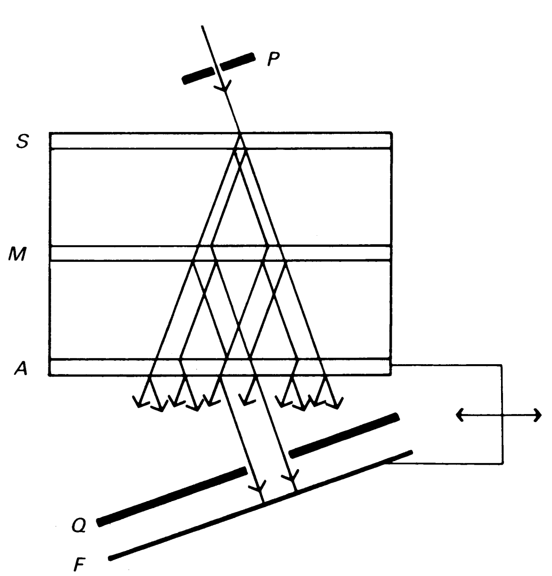

Fig. 2.7.5.1. Scanning arrangement for moiré topography with the Bonse–Hart interferometer.

2.7.5.2. *Real-time viewing of topograph images*

Position-sensitive detectors involving the production of electrons are described in Chapter 7.1, Sections 7.1.6 and 7.1.7, and Arndt (1986, 1990). Those descriptions cover all the image-forming devices that form the core of systems set up for ‘live’ X-ray topography. Here, discussion is limited to remarks on the historical development of techniques designed for making X-ray topographic images directly visible, and on the leading systems that are now sufficiently developed to be acceptable for routine use, in particular on topograph cameras set up at synchrotron X-ray sources. Two types of system became practicalities about the same time, that using direct conversion of X-rays to electronic signals by means of an X-ray-sensitive vidicon television camera tube (Chikawa & Fujimoto, 1968), and the indirect method using an external X-ray phosphor coupled to a multistage electronic image-intensifier tube (Reifsnider & Green, 1968; Lang & Reifsnider, 1969) or to a television-camera tube incorporating an image-intensifier stage (Meieran, Landre & O’Hara, 1969). These two approaches, the direct and the indirect, remain in competition. Developments up to the middle 1970’s have been comprehensively reviewed by Hartman (1977). Since that time, Si-based, two-dimensional CCD (charge-coupled device) arrays have come into prominence as radiation detectors. They can be used for direct conversion of low-energy X-rays into electronic charges as well as for recording images of phosphor screens. As illustrated by Allinson (1994), four configurations employing CCD arrays for X-ray imaging can be considered: (i) direct detection by the ‘naked’ device; (ii) detection by phosphor coated directly on the CCD array; (iii) phosphor separate, and optically coupled to the CCD by lens or fibre-optics; and (iv) the addition to (iii) of an image intensifier

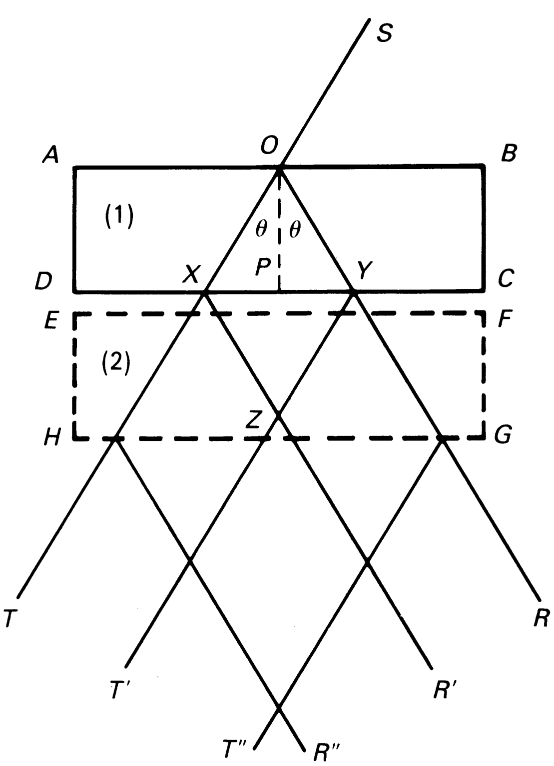

Fig. 2.7.5.2. Superposition of crystals (1) and (2) for production of moiré topographs. [Reproduced from *Diffraction and Imaging Techniques in Material Science*, Vol. II. *Imaging and Diffraction Techniques*, edited by S. Amelinckx, R. Gevers & J. Van Landuyt (1978), Fig. 21, p. 695. Amsterdam, New York, Oxford: North-Holland.]